

PCCP

Accepted Manuscript



This is an *Accepted Manuscript*, which has been through the Royal Society of Chemistry peer review process and has been accepted for publication.

Accepted Manuscripts are published online shortly after acceptance, before technical editing, formatting and proof reading. Using this free service, authors can make their results available to the community, in citable form, before we publish the edited article. We will replace this *Accepted Manuscript* with the edited and formatted *Advance Article* as soon as it is available.

You can find more information about *Accepted Manuscripts* in the [Information for Authors](#).

Please note that technical editing may introduce minor changes to the text and/or graphics, which may alter content. The journal's standard [Terms & Conditions](#) and the [Ethical guidelines](#) still apply. In no event shall the Royal Society of Chemistry be held responsible for any errors or omissions in this *Accepted Manuscript* or any consequences arising from the use of any information it contains.

1-Naphthol as an ESPT Fluorescent Molecular Probe for Sensing Thermotropic Microenvironmental Changes of Pluronic F127 in Aqueous Media

Jitendriya Swain and Ashok Kumar Mishra*

Department of Chemistry, Indian Institute of Technology Madras, Chennai 600 036, India

Abstract

Thermotropic microenvironmental changes and the level of hydration in different microenvironments of pluronic F127 (PF127), (PEO₁₀₆ PPO₇₀ PEO₁₀₆, average molar mass 13,000) in aqueous media have been studied using 1-naphthol, an ESPT fluorescent molecular probe. The appearance of 1-naphthol neutral form fluorescence in aqueous PF127 (10 % w/v) solution indicates the ability of 1-naphthol to sense hydrophobic domain in the micellar aggregation. There is a marked enhancement of the neutral form fluorescence at and above the gelation temperature (20 °C), which shows that the probe can accurately sense the sol-gel transition. In the temperature range 10-40 °C, with increase in temperature there is a progressive enhancement of neutral form fluorescence, blue shift of neutral and anionic form fluorescence, and decrease of deprotonation rate constant (k_{pt}) indicates that water-polymer interfacial region is progressively dehydrated. Since k_{pt} is related to the availability of proton-accepting water in the microenvironments of 1-naphthol, the reduction of k_{pt} implies progressive dehydration. The thermotropic response of I_1/I_3 vibronic band ratio of pyrene-1-butyric acid fluorescence shows progressive increase in the non-polarity of the interfacial domain with increase in temperature. The increase in non-polarity and the decrease of hydration level are strongly correlated.

Introduction:

Excited state proton transfer(ESPT) fluorescent molecular probes are known to be sensitive to the structure and dynamics of microenvironments of different biological and non-biological assemblies.¹⁻⁷ Various ESPT fluorescent probes like 1-naphthol (NpOH), fisetin,

hydroxyflavones, curcumin etc have been extensively studied in different polar and non-polar solvents as well as in the confined environments of organized assemblies.^{1-5,8} There are some fluorescent molecular probes (pyrene, dansyl derivative, anilino naphthalene sulfonic acid, coumarins) known for their ability monitor polarity, micro-viscosity and sol-gel transition of pluronic copolymers.^{9, 10, 11, 31} In the present study, we have used a model ESPT probe, 1-naphthol (NpOH), to study the sol and gel state organizations of pluronicF127 (PF127) copolymer system.

NpOH, a prototype ESPT molecular probe, is a very weak acid in the ground state ($pK_a = 9.2$), but a strong acid ($pK_a^* = 0.4$) in the excited singlet state.^{1, 12} In water, NpOH emits from its excited anionic form (NpO^{*-}) at 470 nm whereas in polar nonaqueous media like alcohols, the emission occurs from the neutral form ($NpOH^*$) at ~ 360 nm. The ESPT of NpOH is controlled by the rate at which water relaxes around the ground state and excited state of NpOH in various organized assembly like micelles, cyclodextrin, liposomes and polymers.^{3, 13-19} In water, $NpOH^*$ undergoes fast deprotonation with a decay rate of 35 ps and a corresponding NpO^{*-} fluorescence rise time of 35 ps.²⁰ Robinson et al. proposed that, in solution state, a cluster of ~ 4 water molecules are needed to act as a base for 1-naphthol ESPT.²¹ However, in supersonic jets, no ESPT process is observed even in solvent clusters of NpOH containing more number of water molecules.²² This indicates that the rate of ESPT process in NpOH varies in different microenvironments of organized assembly and solvents mixtures. It is well known that NpOH distributes to hydrophobic microenvironments in organized media such as cyclodextrin, micelles, polymers or liposomes with accompanying ESPT rate retardation, which is reflected in the appearance of $NpOH^*$ fluorescence, the availability of proton accepting water cluster around NpOH being responsible for the phenomenon.^{3, 13-19, 23}

Pluronic F127 (PF127) is a nontoxic, non-ionic amphiphilic molecule composed of hydrophilic poly(ethyleneoxide) (PEO) and hydrophobic poly(propylene oxide) (PPO) triblock polymers (PEO₁₀₆-PPO₇₀-PEO₁₀₆). It has high stability, transparency and thermoreversible gelling ability at room temperature, which make it a suitable vehicle for drug delivery.²⁴⁻²⁶ Generally, pluronics are also used for the solubilization of poorly soluble drug molecules such as carbamazepine, anticancer drugs etc.^{27, 28} The use of PF127 as artificial skin has been reported in the literature.²⁵ Understanding the hydrophilic and hydrophobic multiple microenvironments created by the PF127 block copolymer in the aqueous solution is important for controlling the loading and release mechanism of the different drug molecules. The amphiphilic nature of PF127 makes it both concentration and temperature sensitive.^{29, 30} It is soluble in water below 20 °C, forming low viscous micellar sol state in the concentration range 0.1 % w/v and above 20% (w/v), the micelles organize into cubic structures to form thick non-transparent gels.³⁰ Generally below 20 % of PF127 has been used as drug delivery agent in pharmacology.²⁴ PF127 exhibits the property of reverse thermal gelation characterized by 'lower critical solution temperature' (LCST). At low temperatures (below 20 °C) in aqueous solutions, the PF127 solution is a transparent micellar sol state and at higher temperature (above 20 °C), the polymer chains form a gel structure.^{25, 26} The temperature region between 20-22 °C is the sol to gel phase transition region of PF127.^{29, 30, 31} Self-aggregation of PF127 in aqueous solutions leads to formation of spherical micelles having hydrophobic polypropylene oxide (PPO) cores surrounded by hydrophilic polyethylene oxide (PEO) groups in corona region (< 20 % w/v).³⁰ Literature has shown that micro-heterogeneity, microviscosity and micropolarities of the various regions of the PF127 micelles vary considerably with the variation in temperature.^{29, 30, 31} In this work pluronic F127 (10 %w/v) has been used in a concentration range above CMC and below cubic structure formation which results in transparent hydrogels.

Temperature dependent structural and dynamical changes in aqueous microheterogeneous systems originate from hydrophilic-hydrophobic balance.³⁰ In a sol-gel system such as PF127 that has an LCST, the sol state changes to the gel state because of a conformational change in which the non-polar PPO segments come together and undergo extensive aggregation.²⁴ These processes are accompanied by marked changes in the nature of hydration at the polymer-water interfaces. The sensitivity of NpOH in monitoring interfacial hydration is well known.^{23, 32} Some of the important advantages of NpOH as molecular probe is the ability of NpOH to distribute in both hydrophilic and hydrophobic domains, the large separation of the emission maxima of the two prototropic forms, and the availability of multiple fluorescence decay parameters. These features have been well brought out in a recent study by Mohapatra et al which found that incorporation of bile salt molecules in the bilayer membrane significantly hydrates the membrane even extending to the core of the membrane.²³ Thus monitoring of the thermotropic structural changes of aqueous PF127 system using NpOH as an ESPT fluorescent molecular probe is expected to provide a clearer understanding on the nature of hydration in the microenvironments around the probe in different states of thermotropic aggregation. This is the objective of this work.

Material and Methods

Pluronic F127 (PEO₁₀₆ PPO₇₀ PEO₁₀₆, average molar mass of 13,000) and pyrene-1-butyric acid were purchased from Sigma Chemical Co. (Bangalore, India). 1-Naphthol purchased from SRL, India was recrystallized, sublimed and used after checking its purity. Triple-distilled water was used for the experiments.

Fluorescence emission measurements were performed using Fluoromax-4 fluorescence spectrophotometer. The fluorescence lifetime measurements were carried out using Horiba JobinYvon TCSPC lifetime instrument. 295nm nano-LEDs were used as light source for the experiments with fluorescent probe 1-naphthol. The pulse repetition rate was set to 1 MHz,

and the pulse width was ~ 800 ps for 295 nm LED. The detector response time is less than 1 ns. The instrument response function was collected using a scatterer (Ludox AS40 colloidal silica). The decay data were analyzed using IBH software. Although the value of χ^2 in the range 0.99 – 1.22 is usually considered good, in aqueous polymeric systems the upper range can sometimes be higher. In such cases the lifetime values were accepted if the distribution of residuals were uniform.

Sample preparation

Pluronic F127 solutions were prepared by dissolving accurately weighed amount of the copolymer in 4 μ M probe solution. The final Pluronic F127 concentration in the samples was 10 % (w/v) in water. The samples were left in refrigerator for 1 day for complete dissolution. In this work pluronic F127 (10 % w/v) has been used in a concentration range above CMC and below cubic structure formation which results in transparent hydrogels.³⁰

Results and Discussion:

Fluorescence Intensity of 1-naphthol

Figure 1(A) shows the emission spectra of NpOH in water and in aqueous PF127 (10 %) solutions with the variation in temperature (10 °C-45 °C). The most noticeable feature in the spectra is the appearance of the neutral form NpOH* fluorescence at 360 nm in the PF127 solution and the enhanced intensities of the NpO^{-*} fluorescence at 460 nm. Corresponding to the sol-gel transition at 22 °C, there is a very significant enhancement of NpOH* fluorescence at the expense of NpO^{-*} fluorescence. The other interesting observation is the blue shift of emission maxima. The NpO^{-*} emission in water (470 nm) shifts to 460 nm in PF127 solution in the sol state (<22 °C) and to 450 nm in the gel state (>22 °C). Similarly the NpOH* emission shifts from 360 nm in the sol state to 355 nm in the gel state. Figures 1 (B),

(C) and (D) show these variations explicitly. It is clear that as an ESPT probe, NpOH reflects the sol-gel phase transition temperature accurately.

PF127 (10%) solution shows a very weak intrinsic emission at 345 nm (SIFigure 2). This emission remains constant with temperatures varied from 10 °C to 40 °C (SIFigure 2). At lower temperature (10 °C), NpOH shows a less intense NpOH* emission (Figure 1 A) and it is likely that both NpOH* and PF127 emissions contribute to the observed band at 360 nm (SIFigure 3). With increase in temperature, there is a very significant enhancement of NpOH* emission and thus the contribution from the intrinsic PF127 emission is negligible (SIFigure 3). Fortunately the overlap of PF127 and NpOH* emissions does not pose much problem in the lifetime analysis (discussed subsequently) as the fluorescence lifetime of the intrinsic emission is rather long. There is no intrinsic emission of PF127(10 % w/v) observed above 420 nm (SIFigure 2, 3), thus NpO* emission is uncontaminated.

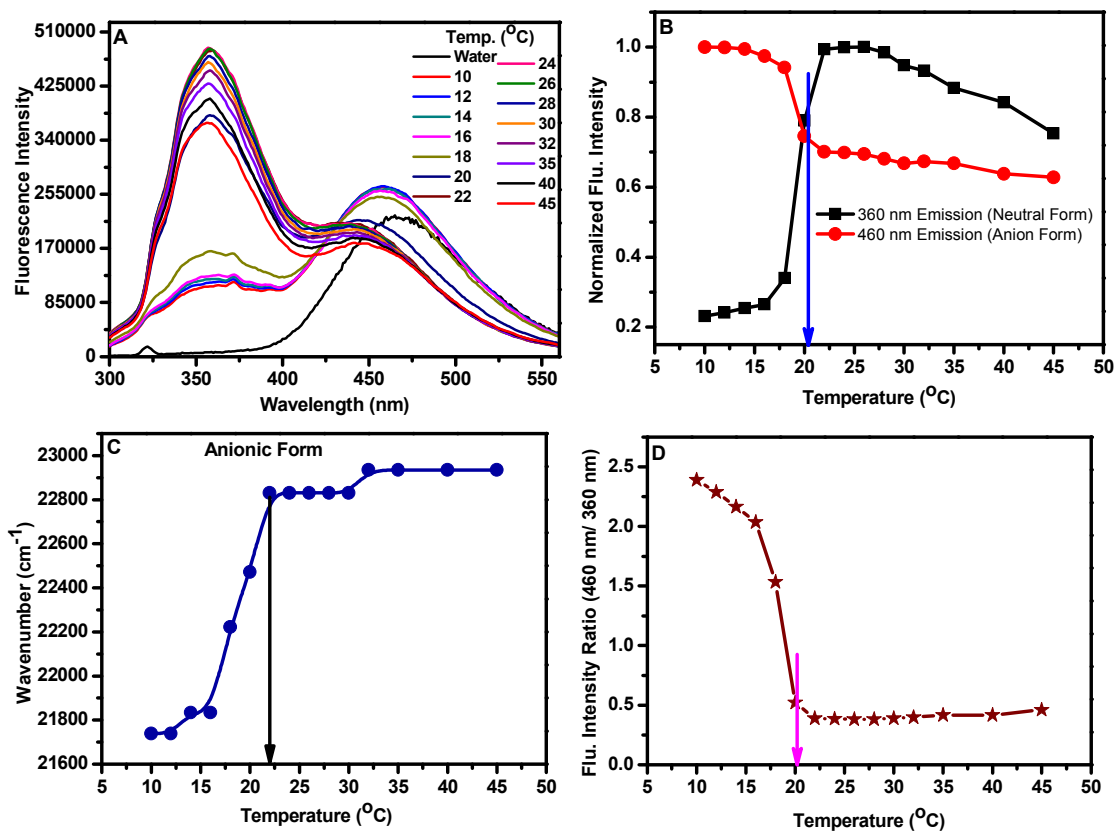


Figure 1. (A) Emission spectra of 1-naphthol in pluronic F127 with varying temperature (B) Plot for the variation of normalized neutral and anion form fluorescence intensities of 1-naphthol in the PF127 in water as a function of temperature. (C) Plot for the variation of anionic form emission maximum (cm^{-1}) of 1-naphthol in PF127 with the variation of temperature. (D) Plot for the fluorescence intensity ratio (460 nm/ 360 nm) of 1-naphthol in PF127 with the variation of temperature. [1-Naphthol]= 4 μM , [PF127] = 10 % (W/v). (Error = 3%)

The blue shift of NpO^{*-} fluorescence with increase in temperature indicates the non-polarity of the microenvironments around NpO^{*-} , the non-polarity being more pronounced in the gel state. Such blue shift is known in the microenvironments of organized assemblies.²³ The concomitant enhancement of NpOH^* emission clearly indicates that the observed non-polarity is due to non-availability of proton-receiving water in the microenvironment that results in the retardation of ESPT rate. The presence of an iso-emissive region further confirms the existence of two-state equilibrium (Figure 1B).

The sol state of aqueous PF127 is characterised by spherical micelles formed from polymeric aggregates. In the micellar structure the hydrophobic PPO segments of the copolymers come together to form core and the hydrophilic PEO segments form a reasonably thick corona region. The dynamics of water present in this region is known to be slower than the bulk water dynamics due to extensive hydration of PEO chain.^{32,33} Since PF127 is thermoreversible with lower LCST, above gelation temperature the PPO segments significantly enhance their aggregation due to hydrophobic association and form hydrogel. In the micellar form, the corona region comprising of PEO segments is sufficiently hydrated.^{9,34} In the gel phase there is a diminished aqueous solubility of the PEO block (corona region) that causes the corona region to shrink.³⁵ The blue shift of NpO^{*-} fluorescence maximum in the sol state as compared to that in water and the further blue shift on gelation is thus a result of increase in hydrophobicity of the microheterogeneous organisation of aqueous PF127. The trends of enhancement of NpOH^* fluorescence can also be understood by similar model.

Since a cluster of 4 water molecules act as base to receive a proton from NpOH^* ,²¹ the enhancement of NpOH^* fluorescence directly correlates with the absence of free water in the microenvironments of the probe. A clearer understanding of the fluorescence intensity of the two prototropic forms requires a detailed analysis of the fluorescence decay dynamics.

Fluorescence Lifetime Studies

Fluorescence lifetime studies were carried out for the neutral form (NpOH^* , $\lambda_{\text{em}} 360 \text{ nm}$) as well as the anion form (NpO^-* , $\lambda_{\text{em}} 460 \text{ nm}$) of 1-naphthol in PF127 with increase in temperature from 10°C to 40°C . In water, the fluorescence lifetime of NpO^-* at 460 nm is 8 ns and the fluorescence lifetime of NpOH^* at 360 nm is 35 ps .^{20, 23} In PF127 solution, NpO^-* fluorescence decay has a biexponential fit till 20°C and then above 20°C , it shows a tri exponential fit with a rise time of $3\text{-}4 \text{ ns}$ (Figure 2 A, Table 1, SI Figure 4). The lifetime of NpOH^* exhibits a tri-exponential fit with the increase in temperature from 10°C to 40°C in PF127 (Figure 2 B, Table 2, SI Figure 5).

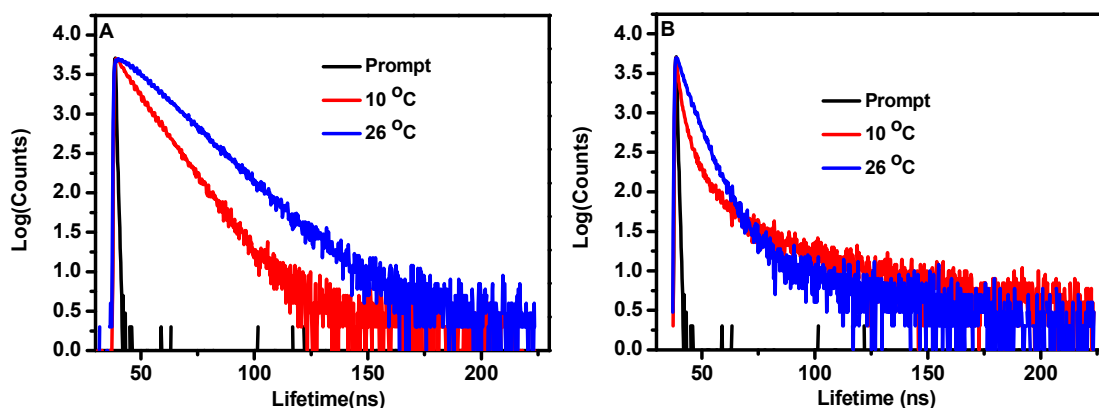


Figure 2. Plot for the fluorescence lifetime decay profile of 1-naphthol in PF127 at different temperature 10°C and 26°C (A) anionic form (460 nm), (B) neutral form (360 nm). ($[\text{1-naphthol}] = 4 \mu\text{M}$, $[\text{PF127}] = 10 \%$ (w/v), ($\lambda_{\text{ex}} = 290 \text{ nm}$).

Table 1. Variation in fluorescence lifetimes and amplitudes of NpO^{*-} with the increase in temperature in PF127. $\lambda_{\text{ex}} = 295 \text{ nm}$, $\lambda_{\text{em}} = 460 \text{ nm}$, $[\text{1-naphthol}] = 4 \mu\text{M}$, $[\text{PF127}] = 10 \%$ (w/v). The corresponding residue distribution plots with the variation of temperature given in SI Figure 6. (Error = 3%)

Em=460 nm Temp. (°C)	τ_{a1} (ns)(B_{a1}) Rise Time	τ_{a2} (ns)(B_{a2}) (Bulk water)	τ_{a3} (ns)(B_{a3}) (Hydrophilic Hydrophobic Interphase)	χ^2
10		8.85(0.61)	12.85(0.39)	1.3
12		9.16(0.69)	13.12(0.31)	1.1
14		9.12(0.63)	12.73(0.37)	1.2
16		9.51(0.80)	14.10(0.20)	1.1
18		9.9(0.80)	15.73(0.20)	1.3
20		9.86(0.77)	15.36(0.23)	1.2
22	3.46(-0.47)	8.89(0.07)	17.00(1.39)	1.8
24	3.30(-0.55)	8.73(0.08)	16.84(1.47)	1.8
26	4.70(-0.45)	8.27(0.12)	16.24(1.33)	1.6
30	4.81(-0.51)	8.27(0.17)	16.28(1.34)	1.5
35	4.80(-0.51)	8.20(0.17)	16.30(1.34)	1.5
40	4.23(-0.66)	7.73(0.25)	15.17(1.41)	1.6

The short decay component τ_{a2} of NpO^{*-} is close to the fluorescence lifetime of NpO^{*-} in water (8 ns).²³ Thus τ_{a2} component appears to originate from NpOH present in the bulk water. It may be noted that this lifetime component does not change much over the entire temperature range. Taking cue from the observation that NpO^{*-} emission originating from lipid-water interfaces in liposomes has a lifetime $\sim 15\text{-}20 \text{ ns}$,²³ The longer decay component τ_{a3} can be ascribed to the presence of NpOH at the polymer-water interface. In the sol state, where PF127 is in a micellar aggregate state containing a distinct corona region, the value of τ_{a3} is 13~14 ns. The corona region in pluronic is characterized by the presence of fully hydrated PEO chains immersed in water that has slower dynamics than free bulk water.^{32,33}

In contrast, the motional restriction at the gel state polymer-water interface causes the value of τ_{a3} to increase to ~ 16 ns. The presence of the ~ 4 ns rise time (τ_{a1}) component in the gel state (< 22 °C) is noteworthy as this provides strong evidence for the very slow ESPT rate at the polymer-water interface. The amplitude of this component, B_{a1} , also tends to increase roughly with increasing temperature, although the trend is not uniform. In contrast, B_{a2} , the amplitude corresponding to the population of NpO^{*-} emitting from bulk water keep increasing over the entire temperature range, the value being fairly low at and above gelation temperature. This indicates significant partitioning of NpOH from bulk water to the polymeric microenvironments with increasing temperature.

Table 2. Variation in fluorescence lifetimes, amplitudes and k_{pt} of NpOH^* with the increase in temperature in PF127. $\lambda_{ex} = 295 \text{ nm}, \lambda_{em} = 360 \text{ nm}$, $[1\text{-naphthol}] = 4 \mu\text{M}$, $[\text{PF127}] = 10 \%$ (w/v). The corresponding residue distribution plots with the variation of temperature given in SI Figure 7. (Error = 3%)

Em=360 nm Temp. (°C)	τ_{n1} (ns) B_{n1} (Hydrophilic Hydrophobic Interphase)	τ_{n2} (ns) B_{n2} (Hydrophobic Core medium)	τ_{n3} (ns) B_{n3} Intrinsic PF127 Lifetime	χ^2	k_{pt} ($\times 10^8$) (s) (Hydrophilic Hydrophobic Interphase)
10	1.45(0.82)	5.73(0.16)	33.5(0.012)	1.23	5.5
12	1.46(0.81)	5.74(0.16)	34.78(0.011)	1.10	5.5
14	1.32(0.78)	5.10(0.20)	32.00(0.013)	1.22	5.8
16	1.35(0.79)	5.17(0.19)	31.69(0.011)	1.30	5.8
18	1.43(0.76)	5.64(0.22)	33.85(0.012)	1.29	5.6
20	1.72(0.62)	6.00(0.32)	35.09(0.010)	1.18	4.5
22	3.12(0.44)	6.81(0.55)	38.14(0.002)	1.13	1.9
24	4.16(0.45)	7.18(0.57)	40.32(0.004)	1.20	1.1
26	4.29(0.69)	7.67(0.30)	54.71(0.003)	1.31	1.0
30	4.05(0.69)	7.55(0.30)	62.70(0.003)	1.10	1.1
35	3.86(0.69)	7.13(0.30)	50.74(0.003)	1.20	1.2
40	3.69(0.69)	7.16(0.30)	54.38(0.003)	1.32	1.3

The fluorescence decay of NpOH* in PF127 shows a triexponential fit with a longer lifetime components (τ_{n3}) (33-55 ns) (Table 2). This component is very much similar to the intrinsic fluorescence lifetime of PF127 (10%) (SI Table 1 in the supporting information). The very small amplitudes (B_{n3}) of the τ_{n3} components of the decay at lower temperatures (<20 °C), indicate the negligible contribution from the intrinsic fluorescence of PF127 (10 %) towards NpOH* emission of 1-naphthol (Table 2). With the marked enhancement of NpOH* fluorescence intensity in the gel state, there is a significant decrease of B_{n3} to negligible levels, as expected. The τ_{n2} values at 6-7 ns correspond to the emission of NpOH* in non-aqueous media.³ NpOH* emission from the dry core of lipid bilayer membranes are known to be in a similar range of 6-7 ns τ_{n2} implying that the gel state is fully dry,²³ Thus, this component can be ascribed to the micellar core region in the PF127 sol state and the dry non-polar core of the gel state. NpOH* emission lifetimes <5 ns imply the availability of proton-receiving water around the molecule. Thus in lipid bilayer membranes, NpOH* fluorescence lifetime is usually in the range of 1-2 ns.²³ The shorter τ_{n1} lifetime component can be explained in a similar way, originating from the corona region of the sol state and the polymer-water interface. Interestingly, in the gel state, the 3-4 ns decay of NpOH* fluorescence, τ_{n1} , corresponds closely to the fluorescence rise time observed for NpO⁻*. This correspondence as well as the large value of the lifetime clearly indicates that the polymer-water interface of the gel state is rather severely dehydrated.^{32,33} In the sol phase, however the deprotonation rate constant is fairly high. Thus the corresponding anionic rise time is not observable in nano second time domain. The amplitude B_{n2} corresponding to the population of NpOH* present in the dry core region keeps increasing with increasing temperature with a more pronounced increase at sol-gel transition. Since gelation increases the volume of the core domain,^{9, 34} this observation implies increased partitioning of NpOH* to core regions with temperature. B_{n1} reflects the

population of 1-naphthol at the interfacial regions. In the sol state ($<20\text{ }^{\circ}\text{C}$), the presence of a thick corona region in the polymeric micelles can explain the relative large values of B_{n1} . On transition to the gel state ($>20\text{ }^{\circ}\text{C}$), this corona is lost and the polymer-water interface has a much slower water dynamics due to hydrophobic hydration.^{32,33} As a result there is a decrease of B_{n1} .

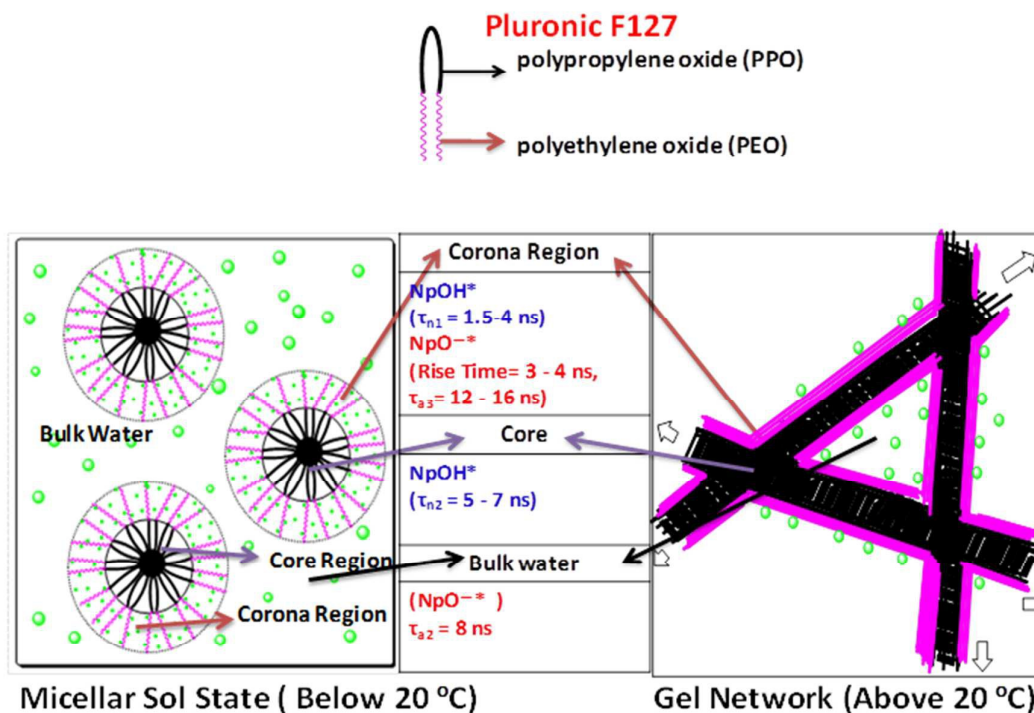
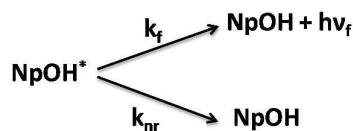


Figure 3. Schematic representation of fluorescence lifetime of both the prototropic form 1-naphthol in the sol and gel state of PF127.

Using the fluorescence decay data of NpO^{-*} , an approximate estimate of the rate constant of proton transfer (k_{pt}) at the interfacial region can be made by using the following simplified mechanism^{4,19}.

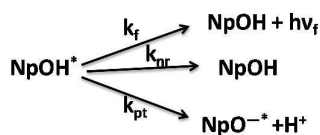
In dry core domains where ESPT is completely inhibited,



$$\tau_{n2} = \frac{1}{k_f + k_{nr}} \dots \dots \dots (1)$$

Where, τ_{n2} is the lifetime of 1-naphthol in the absence of ESPT, k_f is the radiative rate constant, k_{nr} is the non-radiative rate constant.

In the interfacial hydrophilic-hydrophobic domains:



$$\tau_{n1} = \frac{1}{k_f + k_{nr} + k_{pt}} \dots \dots \dots (2)$$

Where, k_{pt} is the rate of proton transfer and τ is the decay time NpOH^* . This scheme assumes the rate constant for the protonation of NpO^{-*} to be negligible. Using the expressions of τ_0 and τ , an expression for k_{pt} giving an approximate estimate would be

$$k_{pt} = \frac{1}{\tau_{n1}} - \frac{1}{\tau_{n2}} \dots \dots \dots (3)$$

The ESPT rate constant of NpOH is strongly dependent on the availability of water around it. The significant decrease in the interfacial hydration of PF127 with increase in temperature from sol state to gel state is reflected in the significant decrease in k_{pt} values (Table 2).

Response of Pyrene-1-butyric Acid Fluorescence to Aqueous PF127 Organization:

As the discussions on response of the ESPT probe NpOH shows, there exists good correspondence between the level of hydration and the polarity in a particular region of a microheterogeneous system like aqueous PF127. The vibronic band ratio I_1/I_3 of pyrene emission is considered a sensitive indicator medium polarity.³⁶⁻³⁹ Taking pyrene-1-butyric

acid (PBA) (SI Figure 1) as a polarity sensitive fluorescent probe that efficiently partitions to the polar-nonpolar interfaces,⁴⁰ a temperature dependent study of the aqueous PF127 system was carried out.

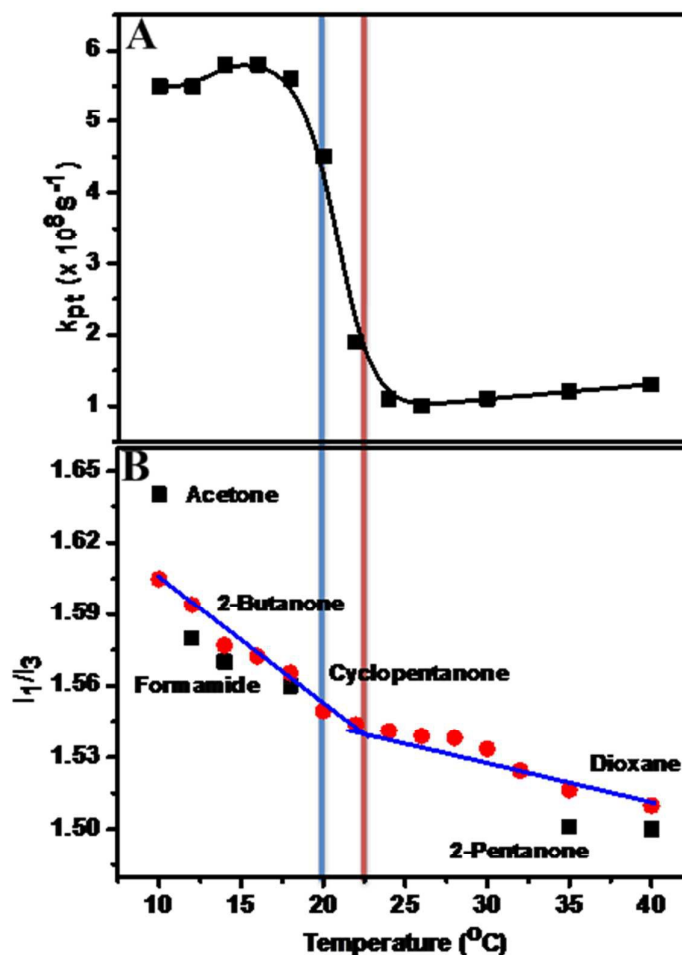


Figure 4. A comparison plot between (A) variation of k_{pt} (corresponding to τ_{n1}) of 1-naphthol in PF127 with the variation of temperature. (B) I_1/I_3 of pyrene-1-butyric acid in PF127 with pyrene emission in different solvents⁴¹ with the variation of temperature. [pyrene butyric acid] = 4 μM , [PF127] = 10 % (W/v). (Error = 3%)

The fluorescence emission of 1-Pyrenebutyric acid overlaps partially with the intrinsic emission of PF127. However the emission intensity of PF127 in the range 370 nm to 390

nm is 150 times lesser (SI Figure 8) than that of PBA. Thus the I_1/I_3 ratio can be used as polarity indicator. Figure 4(B) (SI Figure 9 A, B) shows the variation of vibronic intensity ratio of PBA (I_1/I_3) with temperature. There is a decrease in the intensity ratio with increase in temperature with a break point around 20°C (Figure 4(B), SI Figure 7 B), corresponding to the sol-gel transition. The corresponding data for pyrene⁴¹ in various pure solvents are also given in Figure 4 (B). The progressive decrease in I_1/I_3 values of PBA with increase in temperature and the perceptible break of the variation at sol-gel transition temperature clearly indicates the decrease of the polarity of the interfacial region with increasing temperature. Figure 4 (A, B) correlates the decrease of PBA I_1/I_3 with the decrease of k_{pt} (τ_{n1}) fluorescence lifetime of $NpOH^*$ that originates from the interfacial region. The strikingly similar trend implies that the decrease of the level of hydration of the interface correlates strongly with the increase in the non-polarity of the region. Thus it appears that with increase in temperature, there is a progressive dehydration of the corona region of the sol state as well as the polymer-water interface of the gel state leading to progressive increase in non-polarity. At around the body temperature (37 °C) at which the aqueous PF127 exists in the gel state, the local polarity appears to be fairly low, similar to that of dioxane.

Conclusions

The ESPT dynamics of 1-naphthol is known to be sensitive to the availability proton-accepting water around the microenvironment of the probe, which is reflected in the fluorescence decay dynamics of different prototropic forms of the probe. The present work shows that the fluorescence lifetimes of the excited state anion and neutral form of 1-naphthol enable direct monitoring of the level of hydration in the microenvironments. As 1-naphthol is distributed in all domains of the system: bulk aqueous, interface and hydrophobic dry core, this probe enables complete sensing of all the domains. In addition to the usual fluorescence intensity and spectral shift, the set of lifetime parameters for both the prototropic forms

provide valuable information. With respect to the thermotropic changes observed for aqueous PF127, some of the interesting observations are (i) the sensitive response of the ESPT equilibrium to sol-gel transition, (ii) the progressive decrease of hydration levels with increasing temperature in both sol and gel states, (iii) the observation that the gel core is partially dry and non-polar, (iv) the progressive partitioning of NpOH to the gel microenvironment corresponding to increase in its non-polarity, and (v) the retardation of ESPT at polymer-water interface in the gel state being severe enough so that a long excited state anion rise time is observed.

Supporting Information. Intrinsic fluorescence emission of PF127 (10 % w/v), Fluorescence emission spectra of 1-naphthol in PF127 (10 %) and intrinsic fluorescence emission of PF127 (10 % w/v), fluorescence lifetime decay profile of anionic form (460 nm) and neutral form (360) of 1-naphthol, fluorescence lifetimes and amplitudes of PF127, residue distribution plots for anionic form (460 nm) and neutral form (360) of 1-naphthol in PF127, fluorescence intensity of pyrene-1-butyric acid in PF127.

ACKNOWLEDGMENT

This research was supported by a research project funded by the Department of Science and Technology, Govt. of India. J.S. thanks IIT Madras for his research fellowships.

Reference

1. A. K. Mishra in “*Understanding and Manipulating Excited State Processes*”, *Molecular and Supramolecular Photochemistry Series*, Eds Ramamurthy, V.; Schanze, K. S. Marcel Dekker, Inc., New York, 2001, Chapter 10, **8**, 577.
2. J. Sujatha and A. K. Mishra *Photochem. Photobiol. A*, 1997, **104**, 173-178.
3. J. Sujatha, A. K. Mishra, *Langmuir*, 1998, **14**, 2256-2262.
4. T. Shyamala and A. K. Mishra, *Photochem. Photobio.*, 2004, **80**, 309-315.
5. M. Mohapatra and A. K. Mishra, *J. Phys. Chem. B*, 2011, **115**, 9962–9970.

6. J. Waluk, *Conformational analysis of molecule in excited states*, Wiley-VCH, Weinheim, 2000.
7. A. Muller, (Eds.)“*Electron and proton transfer in chemistry and biology*”,*Studies in physical and theoretical chemistry*, Eds. Ratajczak, H.; Junge, W.; Diemann, E., series 78, Elsevier science publishers B.V..’ Amsterdam, 1992.
8. M. Mouslmani and D. Patra, *RSC Advances*, 2014, **4**, 8316 – 8320.
9. P. Alexandridis, T. Nivaggioli, and T. Alan Hatton, *Langmuir*, 1995, **11**, 1468-1476.
10. U. Anand and S. Mukherjee, *Langmuir*, 2014, **30**, 1014-1021.
11. M. Micutz, E. Matalon, T. Staicu, D. Angelescu, A. M. Ariciu, A. Rogozea, I. M. Turcu and G. Ionita, *New J. Chem.*, 2014, **38**, 2801—2812.
12. J. Sujatha and A. K. Mishra, *J. Fluoresc.* 1997, **7**, 165-168.
13. D. Mandal, S. K. Pal and K. Bhattacharyya, *J. Phys. Chem. A*, 1998, **102**, 9710-9714.
14. R. A. Agbaria, B. Uzank and P. Gill, *J. Phys. Chem.*, 1989, **93**, 3855.
15. D. Sukul, S. K. Pal, D. Mandal, S. Sen and K. Bhattacharyya, *J. Phys. Chem. B*, 2000, **104**, 6128-6132.
16. P. Dutta, A. Halder, S. Mukherjee, P. Sen, S. Sen and K. Bhattacharyya, *Langmuir* 2002, **18**, 7867-7871.
17. A. C. Kumar and A.K. Mishra, *Talanta*, 2007, **71**, 2003–2006
18. Yu. V. Ill’ichev, A. B. Demyashkevich and M. G. Kuzmin, *J. Phys. Chem.*, 1991, **95**, 3438-3444
19. Yu. V. Ill’ichev, A. B. Demyashkevich and M. G. Kuzmin, *Photochem. Photobiol., A* 1993, **74**, 51-63.
20. S. P. Webb, S. W. Yeh, L. A. Philips, M. A. Tolbert and J. H. Clark, *J. Am. Chem. Soc.* 1984, **106**, 7286.
21. G. W. Robinson, P. S. Thistlewaite and J. Lee, *J. Phys. Chem.*, 1986, **90**, 4224.
22. S. K. Kim, S. Li and E. R. Bernstein, *J. Chem. Phys.* 1991, **81**, 3119.
23. M. Mohapatra and A. K. Mishra, *J. Phys. Chem. B*, 2010, **114**, 14934–14940.
24. J. J. Escobar-Chavez, M. Lopez-Cervantes, A. Naik, Y. N. Kalia, D. Quintanar-Guerrero, and A. Ganem-Quintanar, *J Pharm PharmaceutSci*, 2006, **9**, 339-358.
25. M. DiBiase and C. Rhodes, *Drug Develop. Ind. Pharm.*, 1996, **22**, 823-831,
26. J. Gilbert, J. Hadgraft, A. Bye and L. Brookes, *Int. J. Pharm.*, 1986, **32**, 223-228.
27. Y. Kadama, U. Yerramillia and A. Bahadur, *Colloids and Surfaces B: Biointerfaces*, 2009, **72**, 141–147.

28. Z. Wei, J. Hao, S. Yuan, Y. Li, W. Juan, X. Sha and X. Fang, *International Journal of Pharmaceutics*, 2009, **376**, 176–185.
29. K. Nakashima and P. Bahadur, *Adv. Colloid Interface Sci.*, 2006, **123**, 7.
30. B. Chu and Z. Zhou, *Physical Chemistry of Polyoxyalkylene Block Copolymer Surfactants, Nonionic Surfactants: Polyoxyalkylene Block Copolymer Studies*, Marcel-Dekker, Inc., NY, 1996, **60**.
31. M. E. Mohanty, V. J. Rao and A. K. Mishra, *Spectrochimica Acta Part A: Molecular and Biomolecular Spectroscopy*, 2014, **121**, 330–338.
32. Sen, P.; Ghosh, S.; Sahu, K.; Mondal, S. K.; Roy, D.; Bhattacharyya, K.J. *Chem. Phys.* **2006**, *124*, 204905.
33. S. Dey, A. Adhikari, D. K. Das, D. K. Sasmal and K. Bhattacharyya, *J. Phys. Chem. B* 2009, **113**, 959–965.
34. (a) Y. Lin and P. Alexandridis, *J. Phys. Chem. B* 2002, **106**, 10834–10844, (b) I. Goldmints, F. K. von Gottberg, K. A. Smith and T. A. Hatton, *Langmuir*, 1997, **13**, 3659–3664.
35. S. Jeon, S. Granick, K. Kwon, K. Char, *Journal of Polymer Science: Part B: Polymer Physics*, 2002, **40**, 2883–2888.
36. B. Pan, R. Chakraborty and K. A. Berglund, *Journal of Crystal Growth*, 1993, **130**, 587–599.
37. S.A. Latt and S. Brodie, *in: Excited States of Biological Molecules*, Ed. J.B. Burks (Wiley, New York, 1976).
38. F.M. Winnik, *Langmuir*, 1990, **6**, 522.
39. A. N. Diaz, F. G. Sanchez and A. G. Pareja, *Colloids Surfaces A: Physicochem. Eng. Aspects*, 1998, **142**, 27–34.
40. D. Dumas, S. Muller, F. Gouin, F. Baros, M. Viriot and J. Arch. Stoltz, *Biochem. Biophys.* 1997, **341**, 34–39.
41. D. C. Dong and M.A. Winnik, *Can. J. Chem.* 1984, **62**, 2560–2565.